A Dual-Band Circularly Polarized Receiving Antenna for RF Energy Harvesting

Jianxiong Li[1, 2]*, Xiaoming Huang[1, 2], Chunkai Chen[1, 2]
1. School of Electronics and Information Engineering, Tianjin Polytechnic University, Tianjin 300387, China
2. Tianjin Key Laboratory of Optoelectronic Detection Technology and Systems, Tianjin 300387, China
*E-mail: lijianxiong@tjpu.edu.cn

***Abstract*—In this paper, a dual-band circularly polarized antenna at 915 MHz/2.45 GHz is designed. A cascade of a broadband power splitter and a 90° phase shifter is used in the antenna as the dual-feed network. Two concentric square ring radiating patches are coupled fed by the two orthogonally positioned H-shaped slots which are etched in the ground plane. The size of the antenna is 150mm×150mm. The results show that the antenna has the impedance bandwidths of 26.7% and 17.2%, 3-dB axial ratio bandwidths of 8.5% and 16.8% and peak gains of 3.14 dBi and 8.29 dBi at 915 MHz and 2.45 GHz, respectively. Consequently, the proposed antenna meets the requirement of dual-band and circular polarization, and improves the capacity of radio frequency energy harvesting.**

***Index Terms*—Radio frequency energy harvesting, Dual-band, Circular polarization, Antenna**

I. INTRODUCTION

In recent years, the usage of renewable energy for the supply of electronic equipment has been the focus of scientific research. Energy harvesting is the process of collecting ambient energy such as radio frequency (RF), solar, photovoltaic, thermal and mechanical energy and converting the ambient energy into electricity. With the rapid development of wireless communication technologies and the wide application of power sources, such as cellular base station, digital television and wireless router, the ambient RF power density has risen significantly. In contrast to other energy sources, RF energy sources are not limited by weather conditions, indoor or outdoor, and also can reduce the size of the harvesting system and cost. In order to prolong the life of the batteries or avoid using batteries, RF energy harvesting has been applied to portable devices and small electronic devices, e.g. mobile phones, tablet PCs, sensor devices and biomedical implants [1].

RF energy harvesting is derived from the Wireless Power Transmission technology. It converts the RF energy captured from the surrounding environment into available direct current (DC) power by the rectenna technology. Rectenna is the core of RF energy harvesting system, and composed of receiving antenna and rectifier circuit. The performance of receiving antenna will directly affect the capacity of RF energy harvesting. Compared to other power sources, the ambient RF power density is still weak. Therefore, the utilization of multi-band antenna is particularly important to improve the power conversion. For the polarization characteristics of the antenna, since the multipath effects of the electromagnetic waves in the environment can lead to a depolarization phenomenon, the electromagnetic waves have an unknown angle of incidence when entering the antenna, which may reduce the efficiency of the rectenna. In order to maximize the overall efficiency and reduce the polarization loss, it is usually preferred to have an antenna with a circularly polarized characteristic with respect to the design of the receiving antenna. At present, antennas for RF energy harvesting generally have achieved single characteristic of multi-band [2-5] or circular polarization [6], and dual-band circular polarization features with a small frequency ratio [7-8]. A microstrip antenna at 2.45 GHz / 5 GHz was presented in[2]. In [3], a circular patch antenna was used to achieve dual band at 1.95 GHz / 2.45 GHz. In [4], a slot loaded folded dipole antenna was designed to achieve 915 MHz / 2.45 GHz dual-band. In [5], a broadband 1x4 quasi-Yagi antenna array was adopted to realize a dual-band of 1.85 GHz / 2.15 GHz. In [6], a dual-circular polarization at 2.45 GHz was achieved by a square patch antenna with a cross-slot. [7] and [8] separately achieved 2.45 GHz/5.8 GHz, CDMA/GSM band dual-band circular polarization.

Currently, there are only a few antennas that hold the performance of the dual-band circularly polarized at 915 MHz/2.45 GHz. A microstrip line that adopts sequential rotation technique and coaxial cable respectively fed four inverted-F meandered monopole circular arrays and a miniaturized square patch antenna [9]. A serial feed microstrip line coupled diamond-shaped slot to the square ring and cross-slot to the square patch to achieve dual-band [10]. In [11], an aperture coupled antenna was fed by a metamaterial branch-line coupler. The aforementioned antennas have the disadvantage of structural complexity and high cost. In addition, as the radio-frequency identification system operates at 915 MHz / 2.45 GHz, and wireless terminal equipment at 2.45 GHz such as the wireless routers, Bluetooth, laptops are widely used, the frequencies of 915 MHz and 2.45 GHz become the main bands to harvest the ambient RF energy for RF energy harvesting. Therefore, in this paper, an antenna with a simple structure, low-cost and the characteristics of dual-band and circular polarization at 915 MHz and 2.45 GHz, is designed to enhance the capacity of RF energy harvesting.

II. ANTENNA DESIGN

Compared with other types of antenna, microstrip antennas possess advantages of low profile, small volume, light weight, being fabricated together with the feed network, and being massively produced by the printed circuit board technology. Additionally, it is easy to meet the requirements of dual-band, circular polarization and dual polarization [12]. Multi-band antenna can generally be achieved by multi-radiating patch and single radiating patch methods. Multi-radiating patch method refers to a number of radiating patches with different resonant frequencies superimposed to achieve multi-band, while, single radiating patch method means only a single radiating patch is used to achieve multi-band, by the means of reactance loaded or stimulating the work of different resonant modes simultaneously [13]. Although the single radiating patch method is simple, it has the disadvantages of narrow bandwidth and low gain. Thus, multi-radiating patch method is more suitable for the design of broadband, high gain and dual-band antenna. The common realization methods of circular polarization microstrip antenna include single-feed point, multi-feed point and multi-element methods. The single-feed point method generates a pair of orthogonal polarized degenerate modes to radiate circularly polarized waves by the effect of perturbation, without additional feed network; the dual-feed point method excites a pair of orthogonal polarized degenerate modes with equal amplitude and orthogonal phase by a dual-feed network to realize circular polarization. In comparison with the single feed point method, the dual-feed point method can reduce the deterioration of the axial ratio (AR), so the antenna can obtain a wider circularly polarized bandwidth. Multi-elements method refers to using linearly polarized elements for circular polarization radiation [14], which is a microstrip antenna array. This structure is complicated and costly.

It is difficult for single patch loading method to realize the dual-band circular polarization since the big ratio of 2.45 GHz to 915 MHz, which is equal to 2.66. Therefore, in this paper, a stacked multi-patch structure and the dual-feed network are utilized to realize the dual-band and circular polarization performance of the antenna, respectively.

(1) Dual-feed network

This paper adopts a compact feed network with a circuit structure consisting of a broadband 3 dB Wilkinson power splitter [15] and a broadband 90 ° phase shifter [16], which are cascaded to form a 3-port feed network. The structure is shown in "Fig. 1".

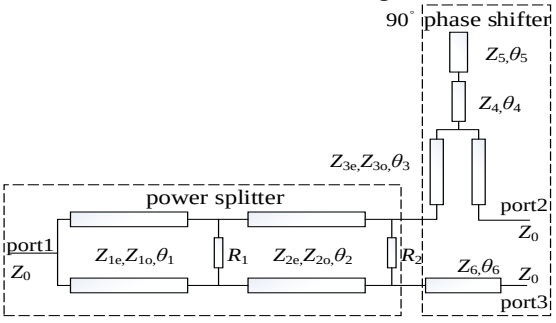

Figure 1. Structure of the dual-feed network

The power splitter consists of two coupled lines and two isolation resistors $R1$ and $R2$. The phase shifter is composed of two paths: one path is the coupled line with a stepped impedance open-ended stub, and the other path is a microstrip transmission line. The even-mode, odd-mode characteristic impedances and electrical lengths of coupled lines are denoted by Z_{ie}, Z_{io}, θ_i (i=1, 2, 3); the characteristic impedances and electrical lengths of microstrip transmission lines are denoted by Z_j, θ_j (j=4, 5, 6), respectively. Z_0=50 Ω is the characteristic impedance of the input and output ports of the feed network. The design parameters of the feed network are calculated by reference to the theoretical formula in [15-16] : Z_{1e}=81.6 Ω, Z_{1o}=43.3 Ω, Z_{2e}=61.3 Ω, Z_{2o}=40.1 Ω, Z_{3e}=41.7 Ω, Z_{3o}=26.1 Ω, Z_4=67.5 Ω, Z_5=22.5 Ω, Z_6=50 Ω, $\theta_1=\theta_2=\theta_3=\theta_4=\theta_5$=90°, θ_6=270°, R_1=63 Ω, R_2=565 Ω.

Simulated and optimized by circuit simulation software Advanced Design System (ADS), the dual-feed network is fabricated on the FR4 substrate with the relative dielectric constant ε_r=4.4, the loss tangent value tanδ=0.02 and the thickness of the substrate $H2$=1.6 mm. The photograph of the fabricated dual-feed network is shown in "Fig. 2". The S parameters and phase difference are measured by the vector network analyzer. The results of simulated and measured S parameters/phase difference of the dual-feed network are shown in "Fig. 3". For the return loss $S11$ below -10 dB, the simulated and measured results are from 800 MHz to 2.53 GHz and from 800 MHz to 2.6 GHz, respectively. In the frequency range of 855 MHz to 2.45 GHz, the simulation and measured transmission coefficients from the input port to the output port $S21$ ($S31$) = -3.8 dB ± 0.5 dB. At two frequency points of 915 MHz and 2.45 GHz, the results of the simulated and measured phase difference between output ports are within the range of 90°±2°.

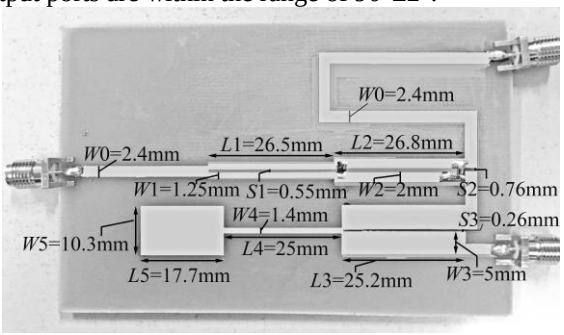

Figure 2. Photograph of the fabricated dual-feed network

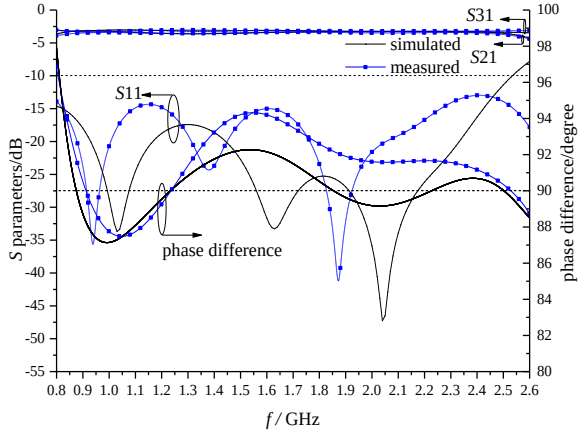

Figure 3. Simulated and measured S parameters /phase difference of the dual-feed network

The results show that the feed network can provide feed signals with equal amplitude and orthogonal phase at 915 MHz and 2.45 GHz, respectively, which lays the basis for the realization of dual-band circularly polarized antenna.

(2) Antenna structure

The proposed antenna is simulated and optimized by the High-Frequency Structure Simulator (HFSS) 15.0. The structure of the antenna and the photograph of the fabricated antenna are shown in "Fig. 4" and "Fig. 5", respectively. Overlooking the antenna, there are successively radiating patches, air layer, a ground plane with two orthogonally positioned H-shaped slots [17], dielectric substrate and feed network. Two concentric square ring aluminum sheets are used as radiating patches with the thickness of $H1$ = 1 mm. The outer and inner sides of a large square ring radiating patch are $W6$=107 mm and $W7$=67 mm for the resonant frequency at 915 MHz, the outer and inner sides of small square ring radiating patch are $W8$=41 mm and $W9$=21 mm for the resonant frequency at 2.45 GHz. The ground plane is printed on the upper surface of the FR4 dielectric substrate by the printed circuit board technique. The H-shaped slot consists of a transverse slot (width $A1$=2 mm, length $B1$=24 mm) and two longitudinal slots (width Ai, length Bi, i=2, 3, where $A2$=3 mm, $B2$=15 mm, $A3$=3 mm, $B3$=14 mm). The coupling strength of the gap between the two patches and the feed network is changed by adjusting the length and width of the H-shaped slot. There is an air layer with the height of H=7 mm between the patches and the ground plane, which can increase the bandwidth of antenna and enhance the antenna gain. The feed network is etched on the lower surface of the dielectric substrate, of which feed ports are directly below the H-shaped slot and located at the middle of the gap between the two rings. The distance from the ports to the center point O of the dielectric substrate is L = ($W7$ + $W8$) / 4 = 27 mm. Two radiating patches are coupled fed through the slots and the air layer. To obtain the impedance matching, the stub with the length of $D1$+$D2$=23 mm is extended in the feeding port. Finally, according to the design parameters, the antenna is fabricated and shown in "Fig. 5".

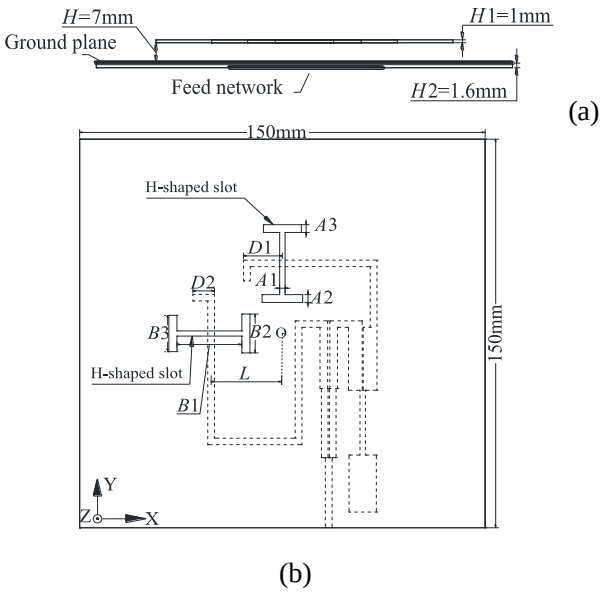

Figure 4. Structure of the proposed antenna. (a) Side view. (b) Feeding dielectric layer

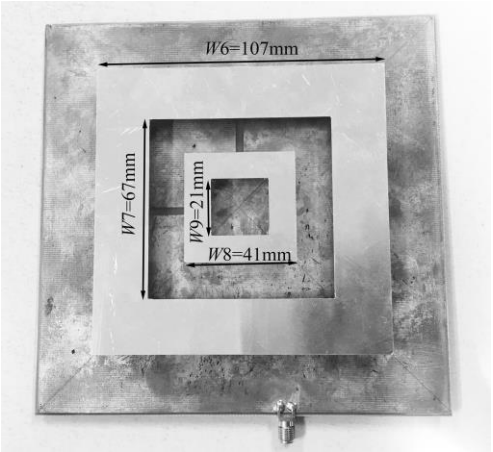

Figure 5. Photograph of the fabricated antenna

III. ANALYSIS OF ANTENNA SIMULATION AND MEASUREMENT RESULTS

The $S11$ parameter of the fabricated antenna is measured by Agilent E5070B vector network analyzer. The simulation and measurement results of the $S11$ parameter of the antenna are shown in "Fig. 6". For $S11$ below -10 dB, the simulated relative impedance bandwidths (IBW) are 29.8% from 703 MHz to 949 MHz for the lower band and 10.9% from 2.354 GHz to 2.626 GHz for the higher band. The simulated $S11$ parameters at the frequency points of 915 MHz and 2.45 GHz are -17.7 dB and -13 dB, respectively. The measured relative impedance bandwidths are 26.7% from 705 MHz to 922 MHz for the lower band and 17.2% from 2.23 GHz to 2.65 GHz for the higher band. The measured $S11$ parameters at the frequency points of 915 MHz and 2.45 GHz are -14.377 dB and -32.351dB, respectively. The proposed antenna covers the dual-band of 915 MHz and 2.45 GHz. The simulation and measurement results are reasonably consistent, but due to the error during the

process of antenna cutting and welding, there is a certain degree of difference.

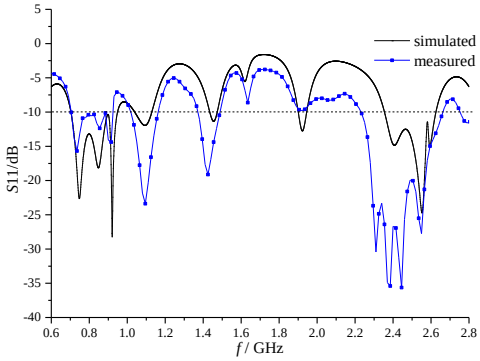

Figure 6. Simulated and measured S11 parameters of the proposed antenna

"Fig. 7" is the antenna gain patterns obtained by simulation. The simulation results show that the peak gain of the antenna at 915 MHz is 3.14 dBi, and the peak gain of the antenna at 2.45 GHz is 8.29 dBi.

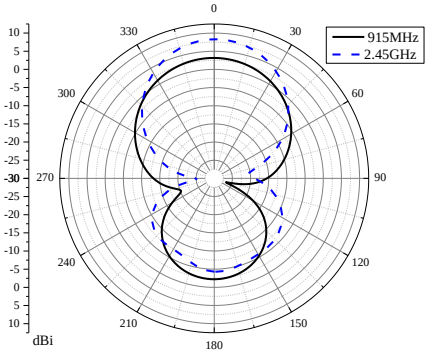

Figure 7. Simulated gain patterns of the proposed antenna

"Fig. 8" is the simulation results of the axial ratio of two frequency bands of 915 MHz and 2.45 GHz. In the simulation results, the axial ratio at the 915 MHz frequency point is 1.71 dB, and that at the 2.45 GHz frequency point is 1.81 dB. The axial ratios are below 3 dB, and the axial ratio bandwidths (ABW) of 915 MHz and 2.45 GHz are 8.5% from 861 MHz to 937 MHz and 16.8% from 2.125 GHz to 2.514 GHz, respectively.

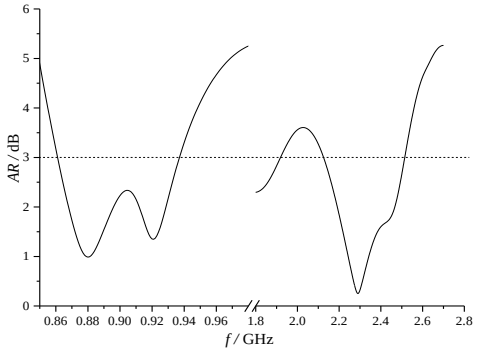

Figure 8. Axial ratio of the proposed antenna

For further evaluating the circularly polarized performance of the proposed antenna, the patterns of the antenna in the xoz and yoz planes are simulated at the two frequency bands at 915 MHz and 2.45 GHz, respectively. "Fig. 9" and "Fig. 10" demonstrate that the cross polarization discriminations of the antenna in the direction of the main radiation at the 915 MHz and 2.45 GHz are 23.3 dB and 22.6 dB separately, which are more than 15 dB, indicating that the antenna has excellent right-hand circular polarization (RHCP) performance at the dual-band 915 MHz and 2.45 GHz.

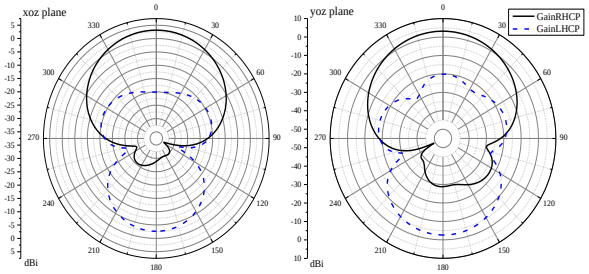

Figure 9. Simulated radiation patterns at 915 MHz in xoz and yoz planes

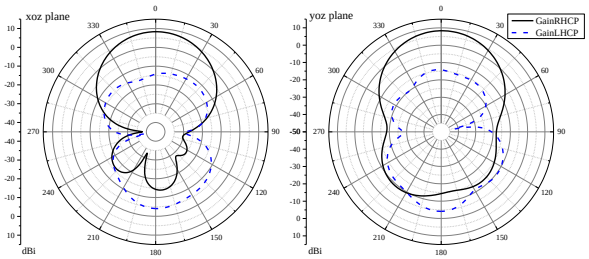

Figure 10. Simulated radiation patterns at 2.45 GHz in xoz and yoz planes

Finally, the proposed dual-band circularly polarized antenna in this paper is compared with the same type of antennas in terms of the impedance bandwidths, axial ratio bandwidths and peak gains. Table 1 shows the comparison results.

TABLE 1
Comparison of antenna performances

Literature	Bands (GHz)	IBW (%)	ABW (%)	Gain (dBi)
[9]	0.915	5	3.1	-0.6
	2.44	3	0.9	1.2
[10]	0.92	4.3	6.5	5
	2.45	10	5.8	9.3
[11]	0.92	2.2	4.4	8.5
	2.45	4.3	8.2	11.4
This paper	0.915	29.8	8.5	3.14
	2.45	10.9	16.8	8.29

It can be seen from the comparison that the antenna impedance bandwidths and the axial ratio bandwidths in

this paper have significant advantages in the same type of antennas. Thus, the antenna designed in this paper has good comprehensive performances.

IV. CONCLUSION

In this paper, a dual-band circularly polarized antenna at 915 MHz / 2.45 GHz is designed for RF energy harvesting. The feed network composes of the broadband coupling Wilkinson power splitter and the broadband phase shifter which provides two feed signals with equal amplitude and orthogonal phase. The antenna with two concentric square ring patches and orthogonal H-shaped coupling slots achieves the desired results of dual-band circular polarization at 915 MHz and 2.45 GHz. The measured relative impedance bandwidths are 26.7% and 17.2%, respectively. The simulated axial ratios are 1.71 dB and 1.81 dB, and the peak gains are 3.14 dBi and 8.29 dBi at 915 MHz and 2.45 GHz, respectively. The antenna designed in this paper has the advantages of easy fabrication, low cost, convenient installation in RF energy harvesting, and can also improve the capacity of radio frequency energy harvesting.

ACKNOWLEDGMENT

This work was supported by the National Natural Science Foundation of China (Grant No. 61372011) and the Tianjin Research Program of Application Foundation and Advanced Technology (Grant No. 15JCYBJC16300).

REFERENCES

[1] Z. M. Zhao, X. D. Wang, "The state-of-the-art and the future trends of electromagnetic energy harvesting," *Diangong Jishu Xuebao/transactions of China Electrotechnical Society*, vol. 30(13), pp. 1-11, 2015.

[2] A. Bakkali, et al, "A Dual-Band Antenna for RF Energy Harvesting Systems in Wireless Sensor Networks," *Journal of Sensors*, (2016-1-14) 2016.11(2016), pp. 1-8, 2016.

[3] M. Ali, A. Abdel-Rahman, A. Allam, et al, "Design of Dual Band Microstrip Antenna with Enhanced Gain for Energy Harvesting Applications," *IEEE Antennas & Wireless Propagation Letters*, issue 99, pp. 1-1, 2017.

[4] K. Niotaki, S. Kim, S. Jeong, et al, "A Compact Dual-Band Rectenna Using Slot-Loaded Dual Band Folded Dipole Antenna," *IEEE Antennas & Wireless Propagation Letters*, vol. 12(1), pp. 1634-1637.

[5] H. Sun, Y. X. Guo, M. He, et al, "A Dual-Band Rectenna Using Broadband Yagi Antenna Array for Ambient RF Power Harvesting." *IEEE Antennas & Wireless Propagation Letters*, vol. 12, pp. 918-921, 2013.

[6] W. Haboubi, H. Takhedmit, J. D. Lan Sun Luk, et al, "An effcient dual-circularly polarized rectenna for RF energy harvesting in the 2.45GHz ISM band," *Progress in Electromagnetics Research*, issue 148, pp. 31-39, 2014.

[7] J. Heikkinen, M. Kivikoski, "A novel dual-frequency circularly polarized rectenna," *IEEE Antennas & Wireless Propagation Letters*, vol. 2(1), pp. 330-333, 2003.

[8] S. Ghosh, A. Chakrabarty, "Dual band circularly polarized monopole antenna design for RF energy harvesting." *IETE Journal of Research*, vol. 62(1), pp. 9-16, 2016.

[9] R. Caso, A. Michel, M. Rodriguez-Pino, "Dual-Band UHF-RFID/WLAN Circularly Polarized Antenna for Portable RFID Readers," *IEEE Transactions on Antennas & Propagation*, vol. 62(5), pp. 2822-2826, 2014.

[10] T. N. Chang, J. M. Lin, "Serial Aperture-Coupled Dual Band Circularly Polarized Antenna," *IEEE Transactions on Antennas & Propagation*, vol. 59(6), pp. 2419-2423, 2011.

[11] Y. K. Jung, B. Lee, "Dual-Band Circularly Polarized Microstrip RFID Reader Antenna Using Metamaterial Branch-Line Coupler," *IEEE Transactions on Antennas & Propagation*, vol. 60(2), pp. 786-791, 2012.

[12] S. S. Zhong, "*Microstrip Antenna Theory and Application*," XIDIAN UNIVERSITY PRESS, pp. 1-172, 1991.

[13] J. W. Zhang, "*Design of Dual-Band and Circularly Polarized Microstrip Antenna*," XIDIAN UNIVERSITY, 2014.

[14] W. Z. Lu, "*Antenna Theory and Techniques*," XIDIAN UNIVERSITY PRESS, pp. 228-258, 2014.

[15] Y. Wu, Y. Liu, Q. Xue, "An Analytical Approach for a Novel Coupled-Line Dual-Band Wilkinson Power Divider," *IEEE Transactions on Microwave Theory and Techniques*, vol. 59(2), pp. 286-294, 2011.

[16] Q. Liu, Y. Liu, J. Shen, et al, "Wideband Single-Layer 90 Phase Shifter Using Stepped Impedance Open Stub and Coupled-Line with Weak Coupling," *IEEE Microwave and Wireless Components Letters*, vol. 24(3) , pp. 176-178, 2014.

[17] S. C. Gao, L. W. Li, M. S. Leong, et al, "Wide-band microstrip antenna with an H-shaped coupling aperture," *IEEE Transactions on Vehicular Technology*, vol. 51(1), pp. 17-27, 2002.